Encapsulated Neutral Ruthenium Catalyst for Substrate-Selective Oxidation of Alcohols

Shaima Hkiri, Maxime Steinmetz, Rachel Schurhammer, David Sémeril

An encapsulated neutral ruthenium catalyst for substrate-selective oxidation of alcohols

Shaima Hkiri,[a] Maxime Steinmetz,[a] Rachel Schurhammer [b] and David Sémeril*[a]

[a] Dr. S. Hkiri, M. Steinmetz, Dr. D. Sémeril
Synthèse Organométallique et Catalyse, UMR-CNRS 7177-Institut de Chimie de Strasbourg
Université de Strasbourg
4 rue Blaise Pascal, 67008 Strasbourg, France
E-mail: demeril@unistra.fr

[b] Prof. R. Schurhammer
Laboratoire de Modélisation et Simulations Moléculaires, UMR-CNRS 7140-Chimie de la Matière Complexe
Université de Strasbourg
4 rue Blaise Pascal, 67008 Strasbourg, France

Supporting information for this article is given via a link at the end of the document.

Abstract: The neutral complex dichloro-{diethyl[(5-phenyl-1,3,4-oxadiazol-2-ylamino)-(4-trifluoro-methylphenyl)methyl]phosphonate} (*p*-cymene)-ruthenium(II) was encapsulated inside a self-assembled hexameric host obtained upon reaction of 2,8,14,20-tetra-undecyl-resorcin[4]arene and water. The formation of an inclusion complex was inferred from a combination of spectral measurements (MS, UV-visible spectroscopy, ^{1}H and DOSY NMR). The ^{31}P and ^{19}F NMR spectra are consistent with motions of the ruthenium complex inside the self-assembled capsule. Molecular dynamics simulations carried out on the inclusion complex confirmed these intra-cavity movements and highlighted possible supramolecular interactions between the ruthenium first coordination sphere ligands and the inner-part (aromatic rings) of the capsule. The embedded ruthenium complex was assessed in the catalytic oxidation (using $NaIO_4$ as oxidant) of mixtures of three arylmethyl alcohols into the corresponding aldehydes. The reaction kinetics were shown to vary as a function of the substrates' size, with the oxidation rate varying in the order benzylalcohol > 4-phenyl-benzylalcohol > 9-anthracenemethanol. Control experiments realized in the absence of hexameric capsule did not allow any discrimination between the substrates.

Introduction

Research in the field of capsule-based architectures has recently become a topic of considerable interest. Capsular objects are not only suitable for the formation of remarkable host-guest complexes, they may also behave as confining spaces that allow for catalytic reactions occurring in a restricted space.[1] With their internal pocket(s), capsular systems thus display similarities with enzymes,[2] and unsurprisingly were already found to modify the chemo-, regio- and stereoselectivity of catalytic reactions with respect to those carried out with classical catalysts operating in bulk solution.[3]

A convenient way to access capsules relies on the self-assembly of macrocyclic, bowl-shaped precursors, such as, for example, pyrogallol[n]arenes and resorcin[n]arenes (n = 4 or 5).[4] Self-assembly processes of this type notably involve equilibria between the precursor molecules, the capsule itself and procapsular fragments so as to facilitate substrate exchange between the interior of the capsule and the external environment.[5]

Originally reported by Atwood *and coll*. in 1997,[6] the self-assembled resorcinarene-based capsule $\mathbf{1}_6$ forms spontaneously in water-saturated organic solvents such as chloroform or benzene, from six macrocycles and eight water molecules (Scheme 1). The structure is held together by a network of 60 hydrogen bonds, involving eight water molecules and the 48 phenolic OH moieties, this resulting in a cavity with an inner volume of 1375 Å^3. In the hexameric capsule $\mathbf{1}_6$, which has an average pKa of 5.9, two types of water molecules can be distinguished: four of them are twice donors and once acceptor of hydrogen bonds; the other four are once donor and twice acceptors of hydrogen bonds. The latter water molecules possess an hydrogen atom that points towards the interior of the capsule, making them suitable for interactions with internal guest molecules while defining an acidic microenvironment characterized by a pKa of 2.5.[7] Recently, the group of Reek demonstrated that in the presence of an excess of water, a second hexameric capsule incorporating 15 water molecules in the hydrogen bonding network is formed. In the latter capsule, a stronger acidity is observed.[8]

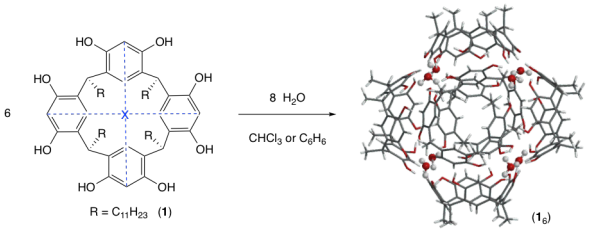

Scheme 1. Self-assembled hexameric capsule based on 2,8,14,20-tetra-undecyl-resorcin[4]arene ($\mathbf{1}_6$) (X represents the center of mass of the resorcinarene **1**).

In recent years, Atwood's hexameric capsule has been successfully used in both organo- or organometallic catalysis.[9] For example, Tiefenbacher *and coll*. reported the 1,4-reduction of *α,β*-unsaturated aldehydes in the presence of proline as the source of chirality. After optimization, owing to noncovalent interactions between the inner walls of the capsule and (chiral) iminium intermediates, the reduced aldehydes were obtained with up to 92 % enantiomeric excess. It is important to note that the same reactions performed in the absence of resorcinarene, and thus of a capsular entity, led to poor enantioselectivity.[10] Although encapsulation of cationic metal complexes such as cobalt,[11] copper,[12] gold,[13] iridium,[14] ruthenium[15] or zinc[12]

have been reported, only few of the corresponding capsular systems were employed in catalysis. Among these are *N*-heterocyclic carbene gold complexes, which were used in competitive hydration of alkynes,[13c] as well as ruthenium complexes suitable for ring closing metathesis.[15b] The confinement of the reported organometallic complexes resulted from π-cation interactions with the inner walls of the cavity.

Recently, we described the synthesis and structure of the ruthenium(II) complex [$RuCl_2$(L)(*p*-cymene)] (**2**) (L = diethyl[(5-phenyl-1,3,4-oxadiazol-2-ylamino)(4-trifluoromethylphenyl) methyl]phosphonate) (Figure 1).[16] As inferred from an X-ray diffraction study this complex has a molecular volume of 818 $Å^3$. We anticipated that an hypothetical capsular complex formed by combining **2** and $\mathbf{1}_6$ would lead to an occupancy factor of 0.59 of the capsule, that is a value close to that defined by Rebek (0.55 ± 0.09) for optimal binding of guests inside hosting capsules.[17] In this context, we report the first immobilization of a neutral ruthenium complex inside the hexameric capsule $\mathbf{1}_6$. The confinement of complex **2** was shown to involve supramolecular interactions between the first coordination sphere ligands and the resorcin[4]arene subunits of $\mathbf{1}_6$. The combination of complex **2** and capsule $\mathbf{1}_6$ was further assessed in the selective catalytic oxidation of primary alcohols into aldehydes.[18]

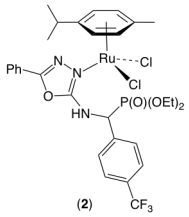

Figure 1. Neutral ruthenium(II) complex employed in the present study.

Results and Discussion

Addition at room temperature of complex **2** to a stirred $CDCl_3$ solution saturated with H_2O of 2,8,14,20-tetra-undecyl-resorcin[4]arene (**1**) ([**1**] = 26 mM and [**2**] = 4 mM) led to the capsular complex $\mathbf{2}\subset\mathbf{1}_6$. In the corresponding ^{1}H NMR spectrum, the $P(O)(OEt)_2$ moieties appeared as two broad signals, respectively at -0.40 and -0.64 ppm. The strong highfield shifts undergone by the EtO signals on going from **2** to $\mathbf{2}\subset\mathbf{1}_6$ reflect the proximity of the EtO groups and aromatic rings of the cavity inner-wall. For its part, the broadness of these signals is a clear indication for the existence of several equilibrating conformers of **2** moving inside $\mathbf{1}_6$.

In order to confirm the formation of a capsular complex, the CH_2CH_3 signals were further used in diffusion-ordered spectroscopy measurements (DOSY). In fact, DOSY experiments revealed the presence a species characterized by a diffusion coefficient of 215 $\mu m^2\ s^{-1}$ (hydrodynamic volume of 21,253 $Å^3$), that can reasonably be assigned to $\mathbf{2}\subset\mathbf{1}_6$ in view of its closeness to the value measured for the hexameric capsule $\mathbf{1}_6$ (216 $\mu m^2\ s^{-1}$; hydrodynamic volume of 21,551 $Å^3$). Noteworthy, there was no evidence of the presence of free ruthenium complex **2** (diffusion coefficient 665 $\mu m^2\ s^{-1}$; hydrodynamic volume of 728 $Å^3$).

As expected, the encapsulation process of complex **2** induced significant changes in the corresponding ^{19}F and ^{31}P NMR spectra. Thus, the well-resolved doublet seen at -62.68 ppm ($^7J_{PF}$ = 2.2 Hz) in the $^{19}F\{^1H\}$ spectrum and the quadruplet at 15.8 ppm ($^7J_{PF}$ = 2.2 Hz) in the $^{31}P\{^1H\}$ NMR spectrum (Figure 2a), both became broad upon encapsulation (signals in the range -62.6/-63.1 for the ^{19}F signal and 16.3/17.4 ppm for the ^{31}P signal) (Figure 2b). These observations indicate possible motions of the complex inside the cavity. Addition of a large excess of NEt_4Cl[19] generated the inclusion complex $NEt_4\subset\mathbf{1}_6$ while releasing the ruthenium complex **2** (Figure 2c), thus illustrating the reversibility of the inclusion process.

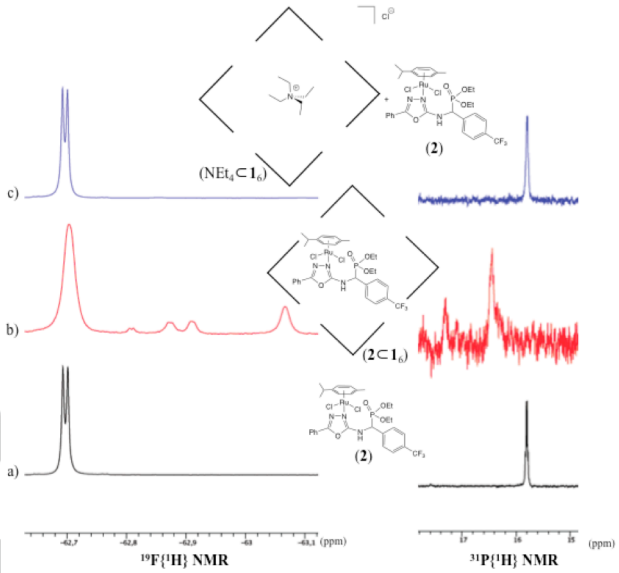

Figure 2. ^{19}F and ^{31}P spectra of free **2** (a), capsular complex $\mathbf{2}\subset\mathbf{1}_6$ (b) and of the mixture obtained after addition of NEt_4Cl to $\mathbf{2}\subset\mathbf{1}_6$ (c).

The electronic absorption spectrum of complex **2** in a water saturated chloroform solution displays a broad low energy band with a maximum at 427 nm ([**2**] = 0.6 mM), which can be attributed to HOMO → LUMO transition with significant d → d character.[20] Addition of 6.5 equivalents of resorcinarene **1** to the previous solution resulted in a slight red shift (12 nm) of the absorption band, consistent with the formation of inclusion complex $\mathbf{2}\subset\mathbf{1}_6$. The observed frequency difference between the free and the inclusion complex lies in the range reported for encapsulated cationic $[Ir(ppy)_2(bpy)]Cl$[14a] and $[Ru(bpy)_3](OTf)_2$[15a] (ppy = 2-phenylpyridinate and bpy = 2,2'-bipyridine) complexes in $\mathbf{1}_6$. As expected, addition of a large excess of NEt_4Cl released the ruthenium complex **2** in solution (λ = 428 nm) and resulted in the complex $NEt_4\subset\mathbf{1}_6$. It should be noted that no change was observed for the absorption maximum on going from the hexameric capsule $\mathbf{1}_6$ to the inclusion complex $NEt_4\subset\mathbf{1}_6$ (Figure 3).

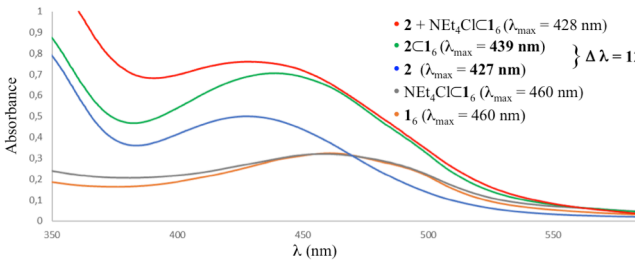

Figure 3. UV-visible measurements of free **2** and inclusion complex $\mathbf{2}\subset\mathbf{1}_6$.

The encapsulation of the ruthenium complex was further analyzed by mass spectrometry (ESI-TOF).[21] Careful analysis of the spectrum revealed the presence of a cation at m/z = 1830.93 ($C_{102}H_{147}O_{12}N_3F_3PClRu$) having exactly the isotopic profile calculated for the cationic species [**2** + **1** - Cl]$^+$. These observations are a clear indication for the affinity of the hexameric capsule for the inorganic complex.

In order to obtain more information on the stabilization of the inclusion complex **2**⊂**1**$_6$, molecular dynamics simulations were performed on the hexameric capsule **1**$_6$ in the absence and in the presence of the ruthenium complex **2**.

Capsule **1**$_6$ was first solvated in a 60 x 60 x 60 Å box containing 2000 and 30 molecules of chloroform and water, respectively. The assembly was simulated over a 10 ns period and in accordance with simulations carried out by Thompson *and coll*.[22] and Reek *and coll*,[8] diffusion of water molecules was observed. During the simulation, approximately twelve molecules of water slowly diffused from the solvent to the inner space generated by the six resorcinarenes (Figures S7 and S8). Molecular dynamics simulations carried out with the ruthenium complex included in capsule **1**$_6$ showed that the neutral ruthenium complex was hosted in the cavity generated by the six resorcinarenes during the whole simulation period (Figure 4).

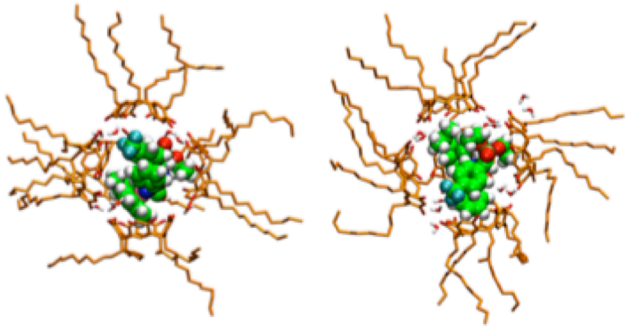

Figure 4. Resorcinarene capsule containing the ruthenium complex **2**. Orthogonal instant views of **2**⊂**1**$_6$ after 5 (left) and 10 ns (right) of dynamics. The front resorcinarene is omitted for clarity.

Consistent with the observations made by NMR, the calculations revealed that the complex is moving inside the capsule, this occurring concomitantly with slight distortions of the supramolecular structure. To evaluate possible size variations of the cavity during these motions, we determined the distances between the pairs of opposite centers of mass of the conical resorcin[4]arene units during the last ns of dynamics. The center of mass was defined as the virtual point located at the intersection of the two segments representing the top rim diameters of the macrocycle (i.e., the segments linking the OC-CH-CO aromatic carbon atoms of opposite resorcinolic rings; Figure 1). In the hexameric capsule **1**$_6$, the three separations were nearly equal (13.2 ± 0.2, 13.2 ± 0.2 and 13.4 ± 0.2 Å; V = 2324 Å^3), in agreement with the symmetrical shape of the capsule structure. The formation of inclusion complex **2**⊂**1**$_6$, whatever the geometrical shape of **2** inside the cavity, induced a slight distortion of the capsule, with two of the above separations shorter than those in the empty capsule (13.0 ± 0.1 and 13.1 ± 0.1 Å) and one longer (13.9 ± 0.1 Å). In contrast, the cavity volume remained practically unchanged (2367 Å^3). A representation of the dynamics of the ruthenium complex **2** inside the capsule is shown in Figure 5.

During the time lapse considered for the simulation, the ligands alternatively interact through weak π•••π,[23] CH•••π[24] and CF•••π[24c, 24d, 25] interactions, all involving the aromatic rings of the six conical resorcin[4]arene units. The various sets of interacting moieties are in equilibrium and contribute to maintaining the complex inside the capsule. Figure 6 shows some typical interactions between ligands of the metal's first coordination sphere and aromatic rings of the resorcinarene units, in particular interactions involving the *p*-cymene π-system (structure A), aromatic protons of the *p*-cymene ring (structure B), CH protons of the P(O)(OEt)$_2$ groups (structure C), the CF$_3$ substituent (structure D), and the phenyl ring linked to the oxadiazole (structure E).

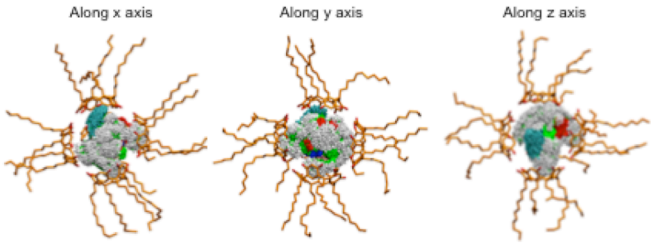

Figure 5. Three-dimensional, cumulated views of the resorcinarene capsule with the ruthenium complex **2** (**2**⊂**1**$_6$). Front resorcinarene is omitted for clarity.

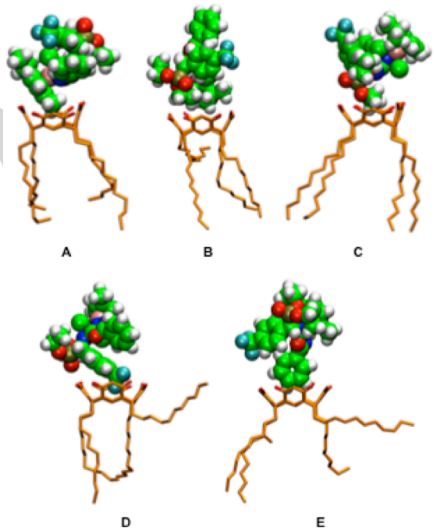

Figure 6. Selected orthogonal views of selected, specific interactions between a resorcinarene unit and complex **2**.

The remarkable selectivity of ruthenium catalysts to a large variety of oxidation reactions motivated us to test the present inclusion arene-ruthenium(II) complex **2**⊂**1**$_6$ as catalyst in the oxidation of primary alcohols into aldehydes.[26]

Oxidation with $NaIO_4$ in the presence of **2**⊂**1**$_6$ led to the formation of a *p*-cymene-free organometallic species characterized by a broad singlet at 18.6 ppm in its $^{31}P\{^1H\}$ NMR spectrum, to which we tentatively attribute the formula **3**⊂**1**$_6$ (Scheme 2).[27] DOSY experiments carried out in $CDCl_3/H_2O$ on the crude product revealed the presence of free *p*-cymene (diffusion coefficient: 1490 μm^2 s^{-1}; hydrodynamic volume: 65 Å^3) as well as that of a much bulkier species (diffusion coefficient of 216 μm^2 s^{-1}; hydrodynamic volume of 21,253 Å^3), namely with a size close to that of **1**$_6$. It is interesting that oxidation of the ruthenium(II) complex **2** into the dioxo-ruthenium(VI) species **3**

did not lead to significant distortion of the hosting hexameric capsule (Scheme 2 and Figures S9-11).

Complex **3** (1 mol %) was assessed in the ruthenium-catalyzed oxidation of primary alcohols and was *in situ* generated from complex **2** and an excess of $NaIO_4$ (2 equiv./substrate; Scheme 3). The catalytic runs were carried out in a $CHCl_3/H_2O$ solvent mixture at 50°C.

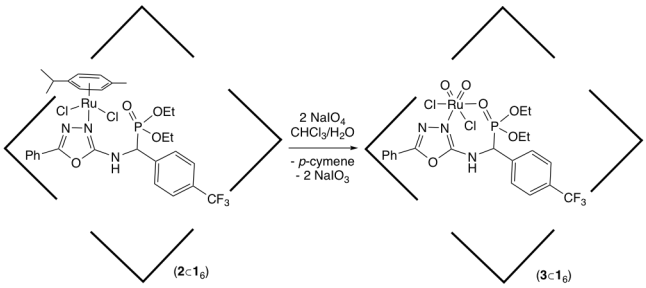

Scheme 2. Formation of the inclusion complex **3**⊂**1**$_6$.

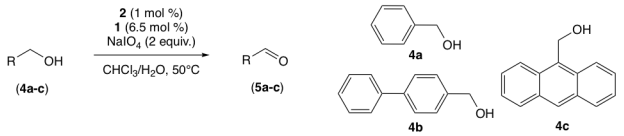

Scheme 3. Ruthenium-catalyzed formation of aldehydes from primary alcohols.

Benzyl alcohol (**4a**) was employed as model substrate. The oxidation tests were carried either in the presence of the hexameric capsule **1**$_6$ alone or that of a mixture of **1**$_6$ and NEt_4Cl (competing guest). The catalytic reactions were monitored by gas chromatography. As seen in Figure 7, which shows the gradual conversion of benzyl alcohol (**4a**) into benzaldehyde (**5a**), encapsulation of the active species **3** (formed by reacting **2** with $NaIO_4$) slowed down the oxidation. Thus, while the conversion of alcohol **4a** was completed after 2 h in the absence of **1**$_6$, full conversion required 8 h in the presence of the capsule. As expected, the use of NEt_4Cl resulted in full conversion after 2 h. Note that in these latter catalytic conditions, no overoxidation of benzaldehyde into benzoic acid was detected. Furthermore, no oxidation of benzyl alcohol was detected when control experiments realized without ruthenium complex **2**, in the presence of $NaIO_4$, were carried out.

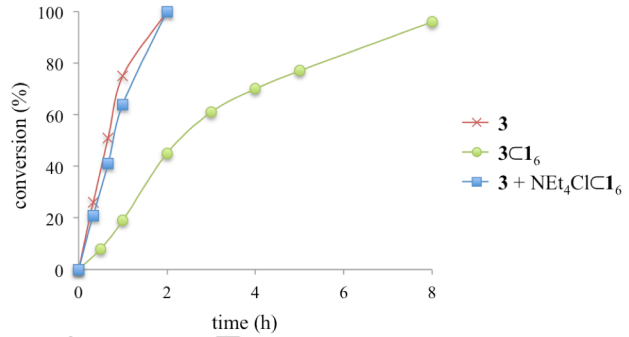

Figure 7. Ruthenium-catalyzed formation of benzaldehyde (**5a**) from benzylalcohol (**4a**). Reaction conditions: **4a** (200 µmol), **2** (2 µmol, 1 mol %) and $NaIO_4$ (400 µmol) in $CHCl_3/H_2O$ (0.6 mL) at 50°C (in red); additional addition of **1** (13 µmol) (in green); additional addition of NEt_4Cl (10 µmol) (in blue).

The ruthenium complex **2**, in association with $NaIO_4$, was further assessed in the competitive oxidation of three arylmethyl alcohols, namely benzylalcohol (**4a**), 4-phenyl-benzylalcohol (**4b**) and 9-anthracenemethanol (**4c**). As expected, when an equimolar mixture of the three alcohols in a chloroform/water mixture was submitted to oxidation in the presence of free **2**, no difference in reactivity between the three alcohols was observed, full conversions being obtained after 2 h at 50°C. In contrast, addition of 2,8,14,20-tetra-undecyl-resorcin[4]arene (**1**) to the alcoholic mixture led to a discrimination of the substrates according to their size.[13c, 28] Thus, the reactivity decreased with the steric hindrance of the reagents, namely in the order benzylalcohol (**4a**) > 4-phenyl-benzylalcohol (**4b**) > 9-anthracenemethanol (**4c**), i.e. in the same order as the occupancy factor of the cavity when the active species **3** and an alcohol were host, the value varies from 58 to 68 % with substrates **4a** and **4c**, respectively. Carrying out the reactions at 50°C, after 5 h conversions of 78, 68 and 53 % were measured for the formation, respectively, of benzaldehyde (**5a**), 4-phenylbenzaldehyde (**5b**) and 9-anthraldehyde (**5c**) (Figure 8).

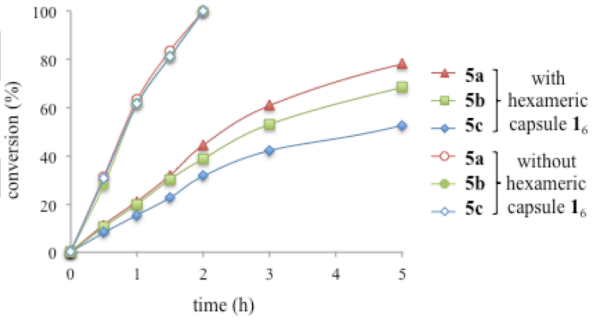

Figure 8. Ruthenium-catalyzed competitive formation of benzaldehyde (**5a**), 4-phenylbenzaldehyde (**5b**) and 9-anthraldehyde (**5c**). Reaction conditions: **2** (2 µmol, 1 mol %), **4a** (66 µmol), **4b** (66 µmol), **4c** (66 µmol) and $NaIO_4$ (400 µmol) in $CDCl_3/H_2O$ (0.6 mL) at 50°C; optional additional addition of **1** (13 µmol).

Conclusion

In summary, we have described the first encapsulation of a neutral arene-ruthenium complex inside a self-assembled hexameric capsule derived from 2,8,14,20-tetra-undecyl-resorcin[4]arene and water. Our findings demonstrate that, unlike a general belief, encapsulation in **1**$_6$ may occur with neutral guests. NMR measurements and molecular dynamics simulations further showed that the encapsulated complex **2** can move inside its host thereby creating a variety of weak interactions involving the ligands and the aromatic rings of cavity wall.

Mixtures of the ruthenium complex **2** and $NaIO_4$ resulted in efficient oxidation catalysts for the conversion of arylmethyl alcohols into the corresponding aldehydes. In the presence of the hexameric capsule **1**$_6$, complex **2** behaved as a size-selective oxidation catalyst towards a ternary mixture of alcohols. Further studies are aimed at exploiting the potential of neutral complexes embedded in supramolecular capsules.

Experimental Section

Diffusion-ordered spectroscopy measurements - Methods

Measurement of self-diffusion coefficients were performed on a BRUKER 600 MHz spectrometer Avance III, equipped with a z gradient probe BBFO, developing a pulsed field gradient of 5 G cm^{-1} A^{-1}. Diffusion NMR data were acquired using a stimulated echo pulse sequence with bipolar z gradients. Limited eddy current delay was fixed to 5 ms. The gradient strength varied linearly, in a random fashion, in 34 experiments. The diffusion time and the duration of the smoothed square gradients were optimized for each sample. Typically the diffusion time was set between 90 and 170 ms, and the half-gradient delay between 900 and 1100 µs. A total recycling time of 5 s was respected between each scans. DOSY spectra were generated with Dynamics Center software from BRUKER using a multi exponential model going up to 3 components. Viscosity and density of $CDCl_3$ saturated with H_2O were measured respectively with an AntonPaar automated microviscometer (AMVn) using a rolling ball and with an AntonPaar DMA500 densitometer using an oscillating U-tube.

Classical molecular dynamics simulations - Methods

The different systems were simulated by classical molecular dynamics (MD) using the AMBER.18 GPU software[29] in which the potential energy U is empirically described by a sum of bond, angle and dihedral deformation energies and a pair wise additive 1-6-12 (electrostatic + van der Waals) interactions between non-bonded atoms.

$$U = \sum_{bonds} k_b(r - r_0)^2 + \sum_{angles} k_\theta(\theta - \theta_0)^2 + \sum_{dihedrals} V_n[1 + cos(n\phi - \gamma)] + \sum_{i=1}^{N-1}\sum_{j=i+1}^{N}\left[\frac{A_{ij}}{R_{ij}^{12}} - \frac{B_{ij}}{R_{ij}^{6}} + \frac{q_i q_j}{\varepsilon_0 r_{i,j}}\right]$$

Each simulated system is composed of six resorcin[4]arene molecules arranged in an a hexameric capsule form unfilled or containing a ruthenium complex **2** solvated by 2000 CH_3Cl molecules and 30 H_2O molecules (box size is around 60 x 60 x 60 Å). Initial structure of the capsule comes from solid state structure published by Atwood.[6] The ruthenium complex has been initially put into the center of the capsule cavity. Two initial conformations were simulated independently and lead to the same conclusions.

Force field parameters for the receptor and the resorcin[4]arene capsule come from the GAFF force field[30] and atomic charges were obtained using the RESP methodology[31] Ruthenium parameters are from Rothlisberger *and coll*.,[32] the catalyst was modeled fully covalent bonded. For CH3Cl we used the model of Kollmann *and coll*.[33] and the TIP3P model for water.[34] Cross terms in van der Waals interactions were constructed using the Lorentz-Berthelot rules. 1-4 van der Waals and 1-4 electrostatic interactions were scaled by a factor of 1.2 and 2, respectively. The MD simulations were performed at 298.15 K starting with random velocities. All simulations have been carried out using 3D Periodic boundary conditions. An atom-based cut-off of 12 Å for non-bonded interactions was applied and long-range electrostatics were calculated using the Ewald summation method in the particle mesh Ewald (PME) approximation, while a long-range correction for vdW interaction was applied.[35]

The different systems were first equilibrated by 0.3 + 0.3 + 0.3 ns of dynamics in the NPT ensemble at respectively 25°K, 100°K and 300°K, followed by 0.3 ns of dynamics in the NVT ensemble. Finally, production runs of at least 10 ns in the NVT ensemble were then simulated. The system temperature was controlled using a Berendsen thermostat with a time step of 1 ps. A time step of 2 fs was used to integrate the equations of motion via the Verlet leapfrog algorithm. Trajectories were saved every 1 ps. Snapshots along the trajectory were taken using the VMD software.[36]

General procedure for the competitive ruthenium-catalyzed oxidation of alcohols

A Schlenk tube was filled with the ruthenium complex **2** (1.5 mg, 2 µmol, 1 mol %), 2,8,14,20-tetra-undecyl-resorcin[4]arene (**1**; 14.4 mg, 13 µmol), $CDCl_3$ (0.5 mL) and H_2O (0.1 mL). The reaction mixture was stirred at room temperature for 45 minutes before addition of benzyl alcohol (**4a**; 7 µL, 66 µmol), 4-biphenylmethanol (**4b**; 12.3 mg, 66 µmol), 9-anthracenemethanol (**4c**; 13.9 mg, 66 µmol) and $NaIO_4$ (85.6 mg, 400 µmol). The reaction was then stirred at 50°C for the desired time. An aliquot of the resulting organic phase was passed through a Milipore filter and analyzed by ^1H NMR spectroscopy.

Acknowledgements

We gratefully acknowledge the University of Carthage and the Tunisian Ministry of Higher Education and Scientific Research for the financial support (grant for S. H.).

Keywords: hexameric capsule • inclusion complex • resorcin[4]arene • ruthenium • homogenous catalysis

[1] a) R. D. M., J. Rebek Jr., *Eur. J. Org. Chem.* **1999**, 1991-2005; b) D. M. Rudkevich, *Chem. Eur. J*. **2000**, *6*, 2679-2686; c) S. J. Dalgarno, N. P. Power, J. L. Atwood, *Coord. Chem. Rev*. **2008**, *252*, 825-841; d) C. J. Brown, F. D. Toste, R. G. Bergman, K. N. Raymond, *Chem. Rev*. **2015**, *115*, 3012-3035; e) K. Kobayashi, M. Yamanaka, *Chem. Soc. Rev*. **2015**, *44*, 449-466; f) C. Deraedt, D. Astruc, *Coord. Chem. Rev*. **2016**, *324*, 106-122; g) A. Galan, P. Ballester, *Chem. Soc. Rev*. **2016**, *45*, 1720-1737; h) G. H. Clever, P. Punt, *Acc. Chem. Res*. **2017**, *50*, 2233-2243; i) J. Yang, B. Chatelet, D. Hérault, J.-P. Dutasta, A. Martinez, *Eur. J. Org. Chem*. **2018**, 5618-5628; j) C. M. Hong, R. G. Bergman, K. N. Raymond, F. D. Toste, *Acc. Chem. Res*. **2018**, *51*, 2447-2455; k) L. J. Jongkind, X. Caumes, A. P. T. Hartendorp, J. N. H. Reek, *Acc. Chem. Res.* **2018**, *51*, 2115-2128; l) S. Roland, J. M. Suarez, M. Sollogoub, *Chem. Eur. J.* **2018**, *24*, 12464-12473; m) V. Mouarrawis, R. Plessius, J. I. van der Vlugt, J. N. H. Reek, *Front. Chem*. **2018**, *6*, 623; n) Y. Fang, J. A. Powell, E. Li, Q. Wang, Z. Perry, A. Kirchon, X. Yang, Z. Xiao, C. Zhu, L. Zhang, F. Huang, H.-C. Zhou, *Chem. Soc. Rev*. **2019**, *48*, 4707-4730; o) I. Némethová, L.-D. Syntrivanis, K. Tiefenbacher, *Chimia* **2020**, *74*, 561-568; p) C. Gaeta, P. La Manna, M. De Rosa, A. Soriente, C. Talotta, P. Neri, *ChemCatChem* **2021**, *13*, 1638-1658; q) G. Olivo, G. Capocasa, D. Del Giudice, O. Lanzalunga, S. Di Stefano, *Chem. Soc. Rev*. **2021**, *50*, 7681-7724.

[2] O. Bristi, O. Reinaud, *Org. Biomol. Chem*. **2015**, *13*, 2849-2865.

[3] a) T. Chavagnan, D. Sémeril, D. Matt, L. Toupet, *Eur. J. Org. Chem*. **2017**, 313-323; b) D. Zhang, K. Jamieson, L. Guy, G. Gao, J.-P. Dutasta, A. Martinez, *Chem. Sci.* **2017**, *8*, 789-794; c) F. Elaieb, S. Sameni, M. Awada, C. Jeunesse, D. Matt, L. Toupet, J. Harrowfield, D. Takeuchi, S. Takano, *Eur. J. Inorg. Chem*. **2019**, 4690-4694; d) N. Noll, F. Werthner, *Chem. Eur. J*. **2021**, *27*, 444-450.

[4] a) T. Gerkensmeier, W. Iwanek, C. Agena, R. Fröhlich, S. Kotila, C. Näther, J. Mattay, *Eur. J. Org. Chem*. **1999**, 2257-2262; b) K. Twum, K. Rissanen, N. K. Beyeh, *Chem. Rec*. **2021**, *21*, 386-395; c) M. Chwastek, P. Cmoch, A. Szumna, *Angew. Chem. Int. Ed*. **2021**, *60*, 4540-4544.

[5] M. Yamanaka, A. Shivanyuk, J. Rebek Jr., *J. Am. Chem. Soc*. **2004**, *126*, 2939-2943.

[6] L. R. MacGillivray, J. L. Atwood, *Nature* **1997**, *389*, 469-472.

[7] P. La Manna, C. Talotta, G. Floresta, M. De Rosa, A. Soriente, A. Rescifina, C. Gaeta, P. Neri, *Angew. Chem. Int. Ed*. **2018**, *57*, 5423-5428.

[8] D. A. Poole, S. Mathew, J. N. H. Reek, *J. Am. Chem. Soc*. **2021**, *143*, 16419-16427.

[9] a) L. Catti, Q. Zhang, K. Tiefenbacher, *Chem. Eur. J*. **2016**, *22*, 9060-9066; b) Q. Zhang, L. Catti, K. Tiefenbacher, *Acc. Chem. Res*. **2018**, *51*, 2107-2114; c) Y. Zhu, J. Rebek Jr., Y. Yu, *Chem. Commun*. **2019**, *55*, 3573-3577; d) C. Gaeta, C. Talotta, M. De Rosa, P. La Manna, A.

Soriente, P. Neri, *Chem. Eur. J.* **2019**, *25*, 4899-4913; e) A. Pappalardo, R. Puglisi, G. T. Sfrazzetto, *Catalysts* **2019**, *9*, 630.

[10] a) T. M. Bräuer, Q. Zhang, K. Tiefenbacher, *Angew. Chem. Int. Ed.* **2016**, *55*, 7698-7701; b) D. Sokolova, K. Tiefenbacher, *RSC Adv*. **2021**, *11*, 24607-24612.

[11] I. Philip, A. E. Kaifer, *J. Org. Chem*. **2005**, *70*, 1558-1564.

[12] T. Zhang, L. Le Corre, O. Reinaud, B. Colasson, *Chem. Eur. J*. **2021**, *27*, 434-443.

[13] a) A. Cavarzan, A. Scarso, P. Sgarbossa, G. Strukul, J. N. H. Reek, *J. Am. Chem. Soc.* **2011**, *133*, 2848-2851; b) L. Adriaenssens, A. Escribano-Cuesta, A. Homs, A. M. Echavarren, P. Ballester, *Eur. J. Org. Chem.* **2013**, 1494-1500; c) A. Cavarzan, J. N. H. Reek, F. Trentin, A. Scarso, G. Strukul, *Catal. Sci. Technol*. **2013**, *3*, 2898-2901; d) A. C. H. Jans, A. Gómez-Suárez, S. P. Nolan, J. N. H. Reek, *Chem. Eur. J.* **2016**, *22*, 14836-14839.

[15] a) S. Horiuchi, H. Tanaka, E. Sakuda, Y. Arikawa, K. Umakoshi, *Chem. Eur. J.* **2016**, *22*, 17533-17537; b) S. Horiuchi, C. Matsuo, E. Sakuda, Y. Arikawa, G. H. Clever, K. Umakoshi, *Dalton Trans*. **2020**, *49*, 8472-8477.

[15] a) G. Bianchini, A. Scarso, G. La Sorella, G. Strukul, *Chem. Commun*. **2012**, *48*, 12082-12084; b) L. J. Jongkind, M. Rahimi, D. Poole, S. J. Ton, D. E. Fogg, J. N. H. Reek, *ChemCatChem* **2020**, *12*, 4019-4023.

[16] S. Hkiri, C. Gourlaouen, S. Touil, A. Samarat, D. Sémeril, *New J. Chem*. **2021**, *45*, 11327-11335.

[17] S. Mecozzi, J. Rebek Jr., *Chem. Eur. J*. **1998**, *4*, 1016-1022.

[18] a) W.-H. Fung, W.-Y. Yu, C.-M. Che, *J. Org. Chem*. **1998**, *63*, 2873-2877; b) P. Singh, A. K. Singh, *Eur. J. Inorg. Chem*. **2010**, 4187-4195; c) R. Ray, S. Chandra, D. Maiti, G. K. Lahiri, *Chem. Eur. J.* **2016**, *22*, 8814-8822; d) J. M. Gichumbi, H. B. Friedrich, B. Omondi, *Inorg. Chim. Acta* **2017**, *456*, 55-63; e) C.-Y. Chern, C.-C. Tseng, R.-H. Hsiao, W. F. F., Y.-S. Kuo, *Heteroat. Chem*. **2019**, 5053702; f) J.-X. Wang, X.-T. Zhou, Q. Han, X.-X. Guo, X.-H. Liu, C. Xue, H.-B. Ji, *New J. Chem*. **2019**, *43*, 19415-19421; g) S. Saranya, R. Ramesh, D. Sémeril, *Organometallics* **2020**, *39*, 3194-3201; h) P. Weingart, P. Hütchen, A. Damone, M. Kohns, H. Hasse, W. R. Thiel, *ChemCatChem* **2020**, *12*, 3919-3928.

[19] A. Shivanyuk, J. Rebek Jr., *Proc. Natl. Acad. Sci*. **2001**, *98*, 7662-7665.

[20] F. Marszaukowski, I. D. L. Guimarães, J. P. da Silva, L. H. da Silveira Lacerda, S. R. de Lazaro, M. P. de Araujo, P. Castellen, T. T. Tominaga, R. T. Boeré, K. Wohnrath, *J. Organomet. Chem*. **2019**, *881*, 66-78.

[21] N. K. Beyeh, M. Kogej, A. Åhman, K. Rissanen, C. A. Schalley, *Angew. Chem. Int. Ed.* **2006**, *45*, 5214-5218.

[22] a) A. Katiyar, J. C. Freire Sovierzoski, P. B. Calio, A. A. Vartia, W. H. Thompson, *Chem. Commun*. **2019**, *55*, 6591-6594; b) A. Katiyar, J. C. Freire Sovierzoski, P. B. Calio, A. A. Vartia, W. H. Thompson, *Phys. Chem. Chem. Phys.* **2020**, *22*, 6167-6175.

[23] a) C. Janiak, J. Chem. Soc., *Dalton Trans*. **2000**, 3885-3896; b) C. R. Martinez, B. L. Iverson, *Chem. Sci*. **2012**, *3*, 2191-2201

[24] a) M. Nishio, *CrystEngComm* **2004**, *6*, 130-158; b) S. Tsuzuki, A. Fujii, *Phys. Chem. Chem. Phys*. **2008**, *10*, 2584-2594; c) W. B. Jennings, N. O'Connell, J. F. Malone, D. R. Boyd, *Org. Biomol. Chem*. **2013**, *11*, 5278-5291; d) X. Xu, B. Pooi, H. Hirao, S. H. Hong, *Angew. Chem. Int. Ed*. **2014**, *53*, 1283-1287.

[25] a) Y. Imai, K. Kamon, K. Kawaguchi, N. Tajima, T. Sato, R. Kuroda, Y. Matsubara, *Lett. Org. Chem*. **2009**, *6*, 588-592; b) D. Chopra, T. N. Guru Row, *CrystEngComm* **2011**, *13*, 2175-2186.

[26] a) E. S. Gore, *Platin. Met. Rev*. **1983**, *27*, 111-125; b) I. W. C. E. Arends, T. Kodama, R. A. Sheldon, *Top. Organomet. Chem*. **2004**, *11*, 277-320; c) S. Muthusamy, N. Kumarswamyreddy, V. Kesavan, S. Chandrasekaran, *Tetrahedron Lett.* **2016**, *57*, 5551-5559.

[27] a) P. Daw, R. Petakamsetty, A. Sarbajna, S. Laha, R. Ramapanicker, J. K. Bera, *J. Am. Chem. Soc*. **2014**, *136*, 13987-13990; b) E. A. Nyawade, H. B. Friedrich, B. Omondi, P. Mpungose, *Organometallics* **2015**, *34*, 4922-4931; c) T. S. Manikandan, R. Ramesh, D. Sémeril, *RSC Adv*. **2016**, *6*, 97107-97115; d) Y.-Q. Zhong, H.-Q. Xiao, X.-Y. Yi, *Dalton Trans.* **2016**, *45*, 18113-18119; e) D. De Joarder, S. Gayen, R. Sarkar, R. Bhattacharya, S. Roy, D. K. Maiti, *J. Org. Chem*. **2019**, *84*, 8468-8480; f) S. Hkiri, S. Touil, A. Samarat, D. Sémeril, *Mol. Catal*. **2022**, *517*, 112014.

[28] a) Q. Zhang, K. Tiefenbacher, *J. Am. Chem. Soc*. **2013**, *135*, 16213-16219; b) E. Lindbäck, S. Dawaigher, K. Wärnmark, *Chem. Eur. J*. **2014**, *20*, 13432-13481; c) L. Catti, K. Tiefenbacher, *Chem. Commun*. **2015**, *51*, 892-894; d) S. Giust, G. La Sorella, L. Sperni, G. Strukul, A. Scarso, *Chem. Commun*. **2015**, *51*, 658-1661; e) T. Chavagnan, C. Bauder, D. Sémeril, D. Matt, L. Toupet, *Eur. J. Org. Chem*. **2017**, 70-76; f) H. Hashimoto, Y. Ueda, K. Takasu, T. Kawabata, *Angew. Chem. Int. Ed.* **2022**, *61*, e202114118.

[29] D. A. Case, I. Y. Ben-Shalom, S. R. Brozell, R. Brozell, D. S. Cerutti T., E. Cheatham I., V. W. D. Cruzeiro, T. A. Darden, R. E. Duke, D. Ghoreishi, M. K. Gilson, H. Gohlke, A. W. Goetz, D. Greene, R. Harris, N. Homeyer, Y. Huang, S. Izadi, A. Kovalenko, T. Kurtzman, T. S. Lee, S. LeGrand, P. Li, C. Lin, J. Liu, T. Luchko, R. Luo, D. J. Mermelstein, K. M. Merz, Y. Miao, G. Monard, C. Nguyen, H. Nguyen, I. Omelyan, A. Onufriev, F. Pan, R. Qi, D. R. Roe, A. Roitberg, C. Sagui, S. Schott-Verdugo, J. Shen, C. L. Simmerling, J. Smith, R. Salomon-Ferrer, J. Swails, R. C. Walker, J. Wang, H. Wei, R. M. Wolf, X. Wu, L. Xiao, D. M. York, P. A. Kollman, *AMBER 18*, University of California, San Francisco **2019**.

[30] J. Wang, R. M. Wolf, J. W. Caldwell, P. A. Kollman, *J. Comput. Chem*. **2004**, *25*, 1157-1174.

[31] C. I. Bayly, P. Cieplak, W. D. Cornell, P. A. Kollman, *J. Phys. Chem*. **1993**, *97*, 10269-10280.

[32] M.-E. Moret, I. Tavernelli, U. Rothlisberger, *J. Phys. Chem. B* **2009**, *113*, 7737-7744.

[33] T. Fox, P. A. Kollman, *J. Phys. Chem. B* **1998**, *102*, 8070-8079.

[34] W. L. Jorgensen, J. Chandrasekhar, J. D. Madura, R. W. Impey, M. L. Klein, *J. Chem. Phys*. **1983**, *79*, 926-935.

[35] M. P. Allen, D. J. Tildesley, *Computer simulation of liquids*, Clarendon Press, Oxford **1987**.

[36] W. Humphrey, A. Dalke, K. Schulten, J. *Mol. Graph*. **1996**, *14*, 33-38.

Entry for the Table of Contents

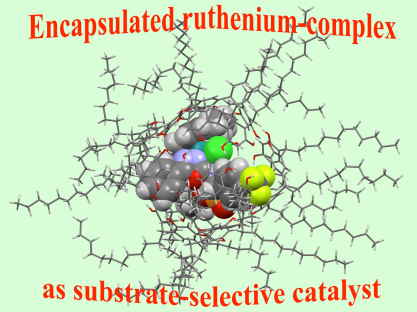

Experimental and theoretical investigations performed on a neutral ruthenium complex immobilized inside a self-assembled hexameric capsule showed that its formation is enabled by supramolecular interactions between the first coordination sphere of the ruthenium and the aromatic rings of the capsule. Substrate size selectivity was observed when the inclusion complex was assessed in the catalytic oxidation of alcohols.